ISSN 0884-5913, Kinematics and Physics of Celestial Bodies, 2017, Vol. 33, No. 3, pp. 122–129. © Allerton Press, Inc., 2017.
Original Russian Text © E.I. Kryuchkov, O.K. Cheremnykh, A.K. Fedorenko, 2017, published in Kinematika i Fizika Nebesnykh Tel, 2017, Vol. 33, No. 3, pp. 41–53.

DYNAMICS AND PHYSICS OF BODIES OF THE SOLAR SYSTEM

Properties of Acoustic-Gravity Waves in the Earth's Polar Thermosphere

E. I. Kryuchkov, O. K. Cheremnykh*, and A. K. Fedorenko**

Space Research Institute, National Academy of Sciences of Ukraine and State Space Agency of Ukraine, Kyiv, 03680 Ukraine

**e-mail: oleg.cheremnykh@gmail.com*

***e-mail: aurora28@i.ua*

Received June 16, 2016

Abstract—The properties of acoustic-gravity waves in the polar regions of the Earth's thermosphere have been studied. It has been shown that the change in AGW amplitudes occurs against the background of large-scale rotational movements of the medium in the polar thermosphere. The amplitudes of waves increase with AGW propagation against the motion of the medium and decrease when AGW propagate along rotation. An analytical expression for the gain coefficient of AGW perturbations is obtained; the wave's amplification effect in the opposite wind given the characteristic parameters of the thermosphere is estimated. The results are consistent with the measurements of AGW parameters in the polar regions from the "Dynamic Explorer 2" satellite.

DOI: 10.3103/S0884591317030047

INTRODUCTION

Acoustic-gravity waves (AGW) play an important role in the dynamics of planetary atmospheres and, to a great extent, determine many processes in the Earth's ionosphere. AGW transfer impulse and energy of significant mass of the medium, which leads to occurrence of convection and atmospheric turbulence. Studying AGW is not only of fundamentally scientific but also of a great practical interest. Being the source of irregularities in the atmosphere, these waves can influence "space weather." AGW are important agents of influence "from below," and, according to present views, they form an ionospheric response to the tropospheric and seismic activity. Despite the significant progress in experimental and theoretical studies of these waves [7, 10, 12–14, 17–22], the question of mechanisms of their generation and propagation at ionospheric altitudes remains largely open.

The present paper is primarily concerned with studying the features of AGW propagation in the polar regions of the Earth. The polar thermosphere is characterized by the existence of spatially nonuniform wind motions. The wind circulation in polar regions, conditioned by the absorption of solar ultraviolet radiation, is influenced by ionospheric effects: (1) involvement of the neutral atmosphere into convective motion of the ionospheric plasma and (2) local heating of the atmosphere by precipitating particles and magnetosphere–ionosphere currents in the auroral oval region. Under the influence of these processes, the wind structure in the polar thermosphere is spatially nonuniform and depends not only on the insolation conditions but also on the processes of magnetosphere–ionosphere interaction. Wind velocities in the polar thermosphere reach the maximum possible values for the Earth's atmosphere and equal 300–700 m/s, depending on the geomagnetic activity [15, 16]. It should be noted that such high wind velocities are primarily contributed by the convective component, while the velocities of the gradient wind at thermospheric altitudes usually do not exceed 250 m/s [15].

Against the background of spatially nonuniform motion of the medium, AGWs of large amplitudes (up to 10% in relative variations of density and temperature) are systematically observed in the polar thermosphere. The nonuniformity of the wind velocity allows energy exchange between the waves and the medium [5]; this results in a change in their amplitudes, selective filtration of the frequency spectrum, and existence of specific azimuths of wave propagation relative to the wind.

Observations from the polar satellite "Dynamic Explorer 2" demonstrate a distinct connection between AGW and the wind in the polar regions [7]. This is indicated by the following aspects: (1) the waves propagate opposite the flow, approximately aligning with the current lines; (2) the amplitudes of

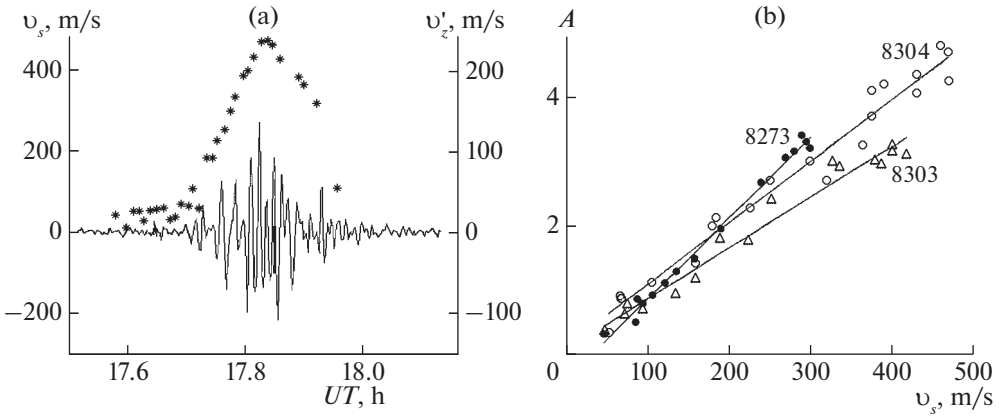

Fig. 1. (a) Meridional wind velocity υ_s (asterisks, left-hand scale) and wave variations of the vertical velocity υ'_z (solid line, right-hand scale) on orbit 8304 of the "Dynamic Explorer 2" satellite; (b) dependence of the amplification coefficient A of the wave amplitude versus the projection of the wind velocity υ_s onto the orbit along passes 8273, 8303, and 8304.

the waves increase simultaneously with an increase in the wind velocity [8, 11]. As an example, Fig. 1a shows the distribution of the meridional wind velocity and wave variations of the vertical velocity of particles along the satellite's orbit 8304. It can be seen that the regions with an increased AGW amplitude spatially match the regions with an increased wind velocity. The dependence of AGW amplitudes versus the projection of the opposing wind velocity onto the satellite orbit is shown in Fig. 1b for several orbit passes.

In order to explain the experimentally observed effect of amplification of AGW amplitudes in the polar thermosphere, we have studied the influence of circulation on propagation of the waves in such a medium. An additional motivation for this research, aside from the abovementioned considerations, are the results of the study [4], where it is shown that acoustic-gravity waves with frequencies close to the Brunt–Väisälä (BV) frequency can occur in the vortex motion of the medium.

MODEL OF HORIZONTAL CIRCULATION

In a general case, vortex motions of the medium are considered in the context of two-dimensionally nonuniform models. Such equations can be solved numerically and, for some specific cases, analytically [1, 9]. Due to the neutral medium being involved in the motion of the ionospheric plasma, a two-vortex system is formed in the polar thermosphere, reflecting the process of magnetospheric convection. The dimensions of these polar vortices at thermospheric altitudes range from several hundreds to approximately 1000 kilometers and wind velocities reach 300–700 m/s [15, 16]. While both vortices are nearly symmetrical in the plasma, as a rule, only one vortex (in the evening sector) is clearly distinct in the neutral medium. This asymmetry is associated with the influence of the Earth's rotation on the formation of vortices: the centrifugal force assists the vortex formation in the evening sector and impedes it in the morning sector. Thus, for simplicity, only one vortex will be considered. Let us specify the following simple model of rotation of the medium. We will assume that the source of circulation is the vortex core located at the center. The vortex dynamics, determined by the processes of magnetosphere–ionosphere interaction, is not considered, assuming the source of rotation to be given. An extended region of vortex-free rotation with the velocity decreasing along the radius is formed behind the core. This is the region that will be considered further. The geometry of intersection of this region by the satellite is schematically shown in Fig. 2.

Despite the relative simplicity of this model, it takes into account such basic features of the polar thermosphere as curvature of motion trajectories of elementary volumes and radial nonuniformity of the velocity. This model makes it possible to bypass many mathematical difficulties typical for two-dimensionally nonuniform vortex models [3]. Earlier, a similar model was studied in [4].

For an isothermal nonviscous atmosphere stratified in the gravity field, the general system of equations of rotational motion of the medium in the cylindrical coordinate system (r, φ, z) with the z axis oriented opposite the gravity force has the following form [6]:

$$\frac{\partial \upsilon_r}{\partial t} + (\vec{\upsilon}\nabla)\upsilon_r - \frac{\upsilon_\varphi^2}{r} = -\frac{1}{\rho}\frac{\partial P}{\partial r}, \tag{1}$$

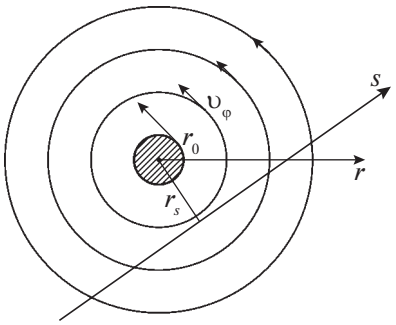

Fig. 2. Schematic visualization of the horizontal circulation region and satellite's orbit *s*: r_0 is the radius of the core and υ_φ is the velocity of medium's rotation.

$$\frac{\partial \upsilon_\varphi}{\partial t} + (\vec{\upsilon}\nabla)\upsilon_\varphi + \frac{\upsilon_r \upsilon_\varphi}{r} = -\frac{1}{\rho r}\frac{\partial P}{\partial \varphi}, \tag{2}$$

$$\frac{\partial \upsilon_z}{\partial t} + (\vec{\upsilon}\nabla)\upsilon_z = -\frac{1}{\rho}\frac{\partial P}{\partial z} - g. \tag{3}$$

We will complement these equations with the matter conservation equation

$$\frac{\partial \rho}{\partial t} + \nabla(\rho\vec{\upsilon}) = 0. \tag{4}$$

and the equation of state

$$\frac{\partial P}{\partial t} + (\vec{\upsilon}\nabla)P = C_s^2\left[\frac{\partial \rho}{\partial t} + (\vec{\upsilon}\nabla)\rho\right]. \tag{5}$$

The following notations are used in the equations: P and ρ are the pressure and density of the medium; υ_r, υ_φ, υ_z are the velocity components; $C_s^2(r) = \gamma\dfrac{P(r)}{\rho(r)} = \gamma g H(r)$ is the speed of sound squared, which, in a general case of rotation, is radius-dependent; γ is the adiabatic index; $H = kT/mg$ is the atmospheric scale height; T is the temperature of the medium; k is the Boltzmann constant; m is the mass of a gas particle; and g is the acceleration of gravity.

Using system (1)–(5), we will study disturbances with the periods of tens of minutes and typical wavelengths on the order of several hundreds of kilometers. For this reason, the summands that describe the Earth's sphericity and the Coriolis force are omitted in the above-mentioned equations, but the force of gravity is taken into account.

Let us consider the stabilized stationary motion of the medium. The vertical stability of such a motion is provided by the hydrostatic equilibrium $\partial P/\partial z = -\rho g$; horizontal stability is provided by the centrifugal force of inertia being compensated by the pressure gradient $\rho\dfrac{\upsilon_\varphi^2}{r} = \dfrac{\partial P}{\partial r}$. As a result, the radial and vertical velocity components of the rotational motion of the medium are equal to zero ($\upsilon_r = \upsilon_z = 0$), and the stationary motion follows the circular horizontal lines of the current.

Behind the vortex core, the circular shifting vortex-free flow with a decreasing velocity is formed [6]:

$$\upsilon_\varphi = V_0\frac{r_0}{r}, \quad r > r_0, \tag{6}$$

where V_0 is the rotational velocity at the edge of the core. Further, we will consider the propagation of wave disturbances in the region behind the core ($r > r_0$), where the velocity of the medium rotation decreases according to law (6).

The $P(r)/\rho(r)$ dependence is determined from the Bernoulli equation for potential flow of compressed gas behind the core [6]:

$$\frac{P}{\rho} = \frac{\gamma-1}{\gamma}\left(\frac{C_\infty^2}{\gamma-1} - \frac{\upsilon_\varphi^2}{2}\right),$$

where C_∞^2 is the speed of sound squared in the resting medium at a distance from the circulation region. For the potential flow behind the vortex core, the P/ρ value is constant not only along the current lines but also throughout the flow region [6]; thus, the radial dependence of the speed of sound has the following form:

$$C_s^2(r) = C_\infty^2 - \frac{\gamma - 1}{2}\upsilon_\varphi^2. \tag{7}$$

It is important for further consideration that this is a weak dependence. The change of $C_s^2(r)$ is maximum near the core's boundary and does not exceed 20% even at the maximum wind velocity $V_0 = 700$ m/s. For this reason, we will assume that the speed of sound is independent of the radius.

AGW IN THE ROTATIONAL FLOW OF THE THERMOSPHERE

Let us investigate the features of the AGW propagation under the assumption of axisymmetry ($d/d\varphi = 0$) of the rotational motion of the atmosphere. Since the system under consideration is uniform in the φ coordinate, then all perturbed values (marked with a prime) will be sought for in the form

$$\begin{aligned}\frac{\upsilon_r'}{V_r} = \frac{\upsilon_\varphi'}{V_\varphi} = \frac{\upsilon_z'}{V_z} = \frac{P'}{P}\\ = \frac{\rho'}{\rho R} = A(r,z)\exp i(\omega t - m\varphi),\end{aligned} \tag{8}$$

where V_r, V_φ, V_z, Π, and R are the amplitude multipliers for perturbed velocities and relative perturbations of pressure and density; $A(r, z)$ is the dimensionless amplitude function (a complex value, in a general case); ω is the frequency in the fixed reference frame (constant); and $k_x = 2\pi/\lambda_x = m/r$ is the component of the wave vector along the $\vec{e}_\varphi$ direction.

From the system of equations (1)–(5) considering (7) and (6), we obtain the linearized equations for free perturbations in the region behind the core:

$$i\bar{\omega}\upsilon_r' - \frac{2\upsilon_\varphi}{r}\upsilon_\varphi' + \frac{\upsilon_\varphi^2}{r}\left(\frac{P'}{P} - \frac{\rho'}{\rho}\right) + \frac{P}{\rho}\frac{d}{dr}\left(\frac{P'}{P}\right) = 0, \tag{9}$$

$$i\bar{\omega}\upsilon_\varphi' + \frac{P}{\rho}\frac{1}{r}\frac{d}{d\varphi}\left(\frac{P'}{P}\right) = 0, \tag{10}$$

$$i\bar{\omega}\upsilon_z' + \frac{P}{\rho}\left(\frac{d}{dz}\frac{P'}{P} + \frac{1}{P}\frac{dP}{dz}\frac{P'}{P}\right) + g\frac{\rho'}{\rho} = 0, \tag{11}$$

$$i\bar{\omega}\frac{\rho'}{\rho} + \frac{1}{r}\frac{d\upsilon_\varphi'}{d\varphi} + \frac{d\upsilon_r'}{dr} + \upsilon_r'\left(\frac{1}{\rho}\frac{d\rho}{dr} + \frac{1}{r}\right) + \frac{d\upsilon_z'}{dz} + \frac{1}{\rho}\frac{d\rho}{dz}\upsilon_z' = 0, \tag{12}$$

$$i\bar{\omega}\frac{\rho'}{\rho} + \frac{1}{r}\frac{d\upsilon_\varphi'}{d\varphi} + \frac{d\upsilon_r'}{dr} + \upsilon_r'\left(\frac{1}{\rho}\frac{d\rho}{dr} + \frac{1}{r}\right) + \frac{d\upsilon_z'}{dz} + \frac{1}{\rho}\frac{d\rho}{dz}\upsilon_z' = 0, \tag{13}$$

The first three equations are the r, φ, z components of the motion equation, respectively; the latter two are obtained from the matter conservation and state equations. In Eqs. (9)–(13), $\bar{\omega} = \omega \pm k_x\upsilon_\varphi$ is the wave frequency in the reference frame moving with the medium. Angle φ is measured in the direction of AGW propagation: the minus sign corresponds to the wave-aligned wind, and the plus sign corresponds to the opposite wind.

It can be seen from Eq. (10) that pressure perturbations P' are in phase with the velocity perturbations υ_φ', which is a typical sign of AGWs that move in the same direction as the particle oscillations in the horizontal plane. In this case, it is the direction of motion along the circular current lines.

Analysis of the satellite data implies that AGWs in polar circulation regions are approximately aligned with the wind directions [8]. Thus, for simplicity, we will consider the waves that propagate along the circular current lines, assuming the possibility of change in their amplitudes along the radius. In this case, $\upsilon_\varphi' = 0$, and dependence on the radius remains only in Eq. (9), which will determine the change in the

AGW amplitude. Substitution of (8) into (9)–(13) yields the system of linear algebraic equations for V_r, V_φ, V_z, Π, and R, which includes the derivatives $\partial A/\partial r$, and $\partial A/\partial z$. Four equations, (10)–(13), are reduced to the square equation

$$\left(\frac{1}{A}\frac{\partial A}{\partial z}\right)^2 - \frac{1}{H}\left(\frac{1}{A}\frac{\partial A}{\partial z}\right) + \frac{\bar{\omega}^2}{C_s^2} + k_x^2\left(\frac{N^2}{\bar{\omega}^2} - 1\right) = 0, \tag{14}$$

where $N^2 = \dfrac{g}{H}\dfrac{\gamma - 1}{\gamma}$ is the Brunt–Väisälä frequency squared. From Eq. (14) we obtain

$$\frac{1}{A}\frac{\partial A}{\partial z} = \frac{1}{2H} \pm ik_z.$$

Let us assume $A(z) = \exp(-iK_z z)$, where $K_z = k_z + i\hat{k}_z$. Then, $\hat{k}_z = \dfrac{1}{2H}$, and k_z is defined by the dispersion

$$k_z^2 = k_x^2\left(\frac{N^2}{\bar{\omega}^2} - 1\right) + \frac{\bar{\omega}^2}{C_s^2} - \frac{1}{4H^2}, \tag{15}$$

which coincides with Hines' equation in its form [13]. However, in the present model, the AGW spectral parameters in the rotating medium system change along the radius.

Since, in our model, the waves do not propagate along the radius ($\upsilon_r' = 0$, $k_r = 0$), the perturbations ρ' and P' determined from system (10)–(13) should be in phase:

$$\gamma\frac{\rho'}{\rho} = \alpha\frac{P'}{P},$$

where

$$\alpha = \left\{\frac{1}{4H^2}\frac{(2-\gamma)}{\gamma}\left[1 - \frac{2(\gamma-1)}{\gamma}\frac{C_s^2}{\bar{U}_x^2}\right] + k_z^2\right\}\left(\frac{1}{4H^2}\left(\frac{2-\gamma}{\gamma}\right)^2 + k_z^2\right)^{-1},$$

and $\bar{U}_x$ is the horizontal phase velocity of AGW in the reference frame of the moving medium.

Then, from Eq. (9), for the coefficient of the amplitude change along the radius, we obtain

$$\frac{1}{A}\frac{\partial A}{\partial r} = \frac{2\upsilon_\varphi}{\bar{U}_x r} - \frac{(\gamma - \alpha)\upsilon_\varphi^2}{C_s^2 r}. \tag{16}$$

The radial dependence of the AGW horizontal phase velocity in the reference frame of the moving medium, which will be used for integration of (16), has the following form:

$$\bar{U}_x(r) = \frac{\bar{\omega}}{k_x} = \frac{\omega r}{m} \pm \frac{V_0 r_0}{r}, \tag{17}$$

where the upper sign corresponds to the opposite wind and the lower sign to the favorable wind.

It should be noted that Eqs. (1)–(5), (9)–(13), and (16) are written in the reference frame of the fixed observer. Dispersion equation (15) sets the connection between the frequency $\bar{\omega}(r) = \omega \pm k_x\upsilon_\varphi$ and components k_x, k_z in the reference frame of the moving medium. Equation (17) basically reflects the connection of AGW phase velocities in the fixed and moving reference frames in the circular geometry of our problem.

INTENSIFICATION OF THE WAVE AMPLITUDE

The expression for the coefficient of the AGW amplitude change along the radius is obtained by integrating Eq. (16) considering the radial dependence (17):

$$A(r) = \left(\frac{\bar{U}_x}{\bar{U}_x \mp \upsilon_\varphi}\right)\exp\left(\frac{\gamma - \alpha}{2}\frac{\upsilon_\varphi^2}{C_s^2}\right) = \left(1 \pm \frac{V_0}{\bar{U}_{x0} \mp V_0}\frac{r_0^2}{r^2}\right)\exp\left(\frac{\gamma - \alpha}{2}\frac{V_0^2}{C_s^2}\frac{r_0^2}{r^2}\right), \tag{18}$$

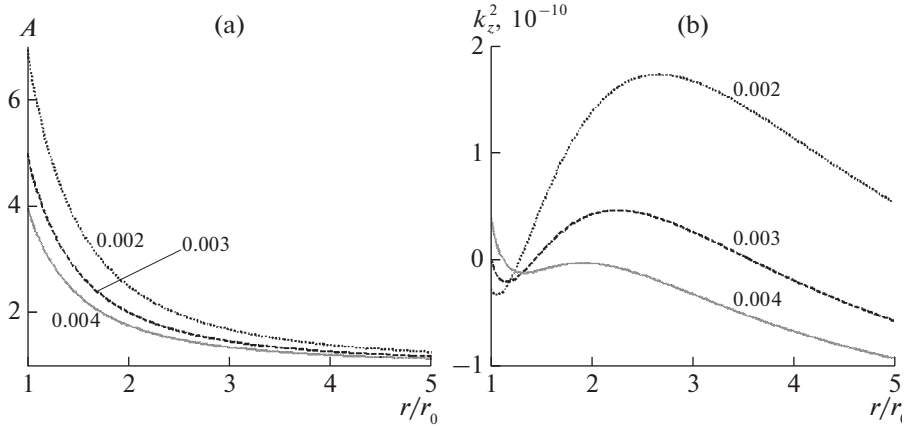

Fig. 3. (a) Amplification coefficient A of AGW amplitude and (b) the k_z^2 value versus radial distance r/r_0: the numbers at the curves are the values of $\omega = 0.002\ s^{-1}$ (period 56 min), $\omega = 0.003\ s^{-1}$ (35 min), $\omega = 0.004\ s^{-1}$ (25 min).

where the upper sign corresponds to the opposite wind and the lower sign to the favorable wind. As immediately seen from (18), the AGW amplitude decreases in the favorable wind and increases in the opposite wind depending on the radius. The exponential multiplier in (18) gives a slight increase in the amplitude of perturbations, which is independent of the wind direction. Even at the maximum value $\upsilon_\varphi = V_0$ at the edge of the core, its value does not exceed 1.3. For the favorable wind, the first multiplier in (18) is always less than 1, which implies a decrease in the AGW amplitude.

It is easy to demonstrate that amplification is primarily provided by the first multiplier, which, in its physical sense, corresponds to the centrifugal forces of inertia (the summand $2\upsilon_\varphi/\bar{U}_x r$ in expression (16)). This immediately follows from the equation of radial force balance $\rho\dfrac{V_\varphi^2}{r} = \dfrac{\partial P}{\partial r}$. Assuming here $V_\varphi = \upsilon_\varphi + \upsilon'_\varphi$, where υ_φ is the unperturbed rotation velocity, we obtain the expression $\rho\dfrac{2\upsilon_\varphi}{r}\upsilon'_\varphi$, for the "wave" part of the centrifugal force of inertia, which is included in (9). Using (10), this summand is transformed to $\rho\dfrac{2\upsilon_\varphi}{\bar{U}_x r}\dfrac{P'}{P}$, and defines the main amplification in Eq. (16).

Without considering the exponential multiplier in expression (18), the change of AGW amplitude along the radius is proportional to the ratio of frequencies: $A(r) \approx \dfrac{\bar{U}_x}{\bar{U}_x \mp \upsilon_\varphi} = \dfrac{\bar{U}_x}{U_x} = \dfrac{\bar{\omega}}{\omega}$. Therefore, those waves are amplified greater in the opposite wind, whose frequency in the reference frame of the medium reaches maximum values ($\bar{\omega}$). Additionally, an increase in AGW amplitudes in rotating medium will be the greater, the smaller the initial frequency ω. The $A(r)$ dependence at different values of periods $T = 2\pi/\omega$ is shown in Fig. 3a. The maximum amplification of AGW amplitudes occurs near the core's boundary and is $A_0 = \bar{U}_{x0}(\bar{U}_{x0} - V_0) \approx 4\ldots9$ for the range of periods from 25 to 60 min. The amplification coefficient significantly increases when the value of the phase velocity of the wave approach the velocity of the flow.

Additional analysis of dispersion (15) shows that the inequality $k_z^2 < 0$ is true near the core's boundary (Fig. 3b), i.e., the waves cannot propagate freely. Basically, this means that the wave train is reflected when the value of the AGW group velocity is equalized with the velocity of the opposite flow. The AGW horizontal group velocity is connected with the horizontal phase velocity via the following relation [2]:

$$\bar{U}_{gx} = \bar{U}_x\frac{\tau^2 - 1}{\tau^2 - u^2}, \tag{19}$$

where $\tau^2 = N^2/\bar{\omega}^2$ and $u^2 = \bar{U}_x^2/C_s^2$. Since, for the gravitational branch $\tau^2 > 1$ and $u^2 < 1$, from (19) it follows that the inequality $\bar{U}_{gx} < \bar{U}_x$ is always true and $\bar{U}_x$ remains greater than υ_φ. Since the group velocity

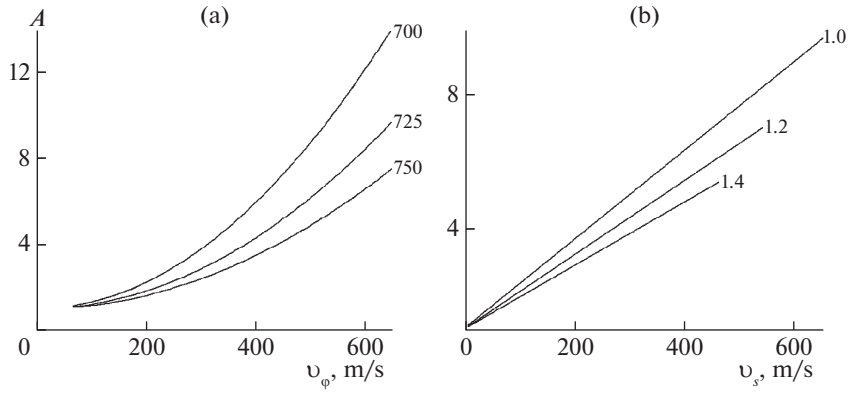

Fig. 4. Dependences of the amplification coefficient A of AGW amplitudes: (a) on υ_φ at $V_0 = 650$ m/s; from top to bottom: $\bar{U}_{x0} = 700$, 725, 750 m/s; (b) on projection of υ_s velocity onto the satellite orbit $\bar{U}_{x0} = 725$ m/s, from top to bottom $n = 1$, 1.2, 1.4.

in AGW is previously compared with the wind velocity, the denominator in (18) cannot be equal to zero. The free propagation of AGW ($k_z^2 > 0$) becomes possible only at some distance from the core's boundary, which depends on ω and V_0 (Fig. 3b). In the range of characteristic AGW frequencies from 0.002 to 0.004 s^{-1}, this distance is $r \approx (1.4...1.7)r_0$ at $V_0 = 600$ m/s. Thus, the observed amplification of amplitude will be slightly less than at the core's boundary. Its value for different frequencies is easily estimated from comparison of Figs. 3a and 3b.

Let us compare the obtained law of amplification (18) with the data of measurements of AGW parameters from the "Dynamic Explorer 2" satellite. As seen from Fig. 1b, the experimental dependence of the wave amplitude on projection υ_s of the opposite wind velocity onto the satellite's orbit is close to linear.

Theoretical dependence $A(\upsilon_\varphi)$ is given in Fig. 4a. It is seen that the calculated curves slightly differ from the experimental ones: the amplitude changes more slowly at relatively low wind velocities and faster at high wind velocities. To bring the theory to closer agreement with the experimental data, we will consider the geometry of intersection of the circulation region by the satellite (Fig. 2). We will obtain the dependence of amplification (18) on projection υ_s by defining this velocity via the relation r_0/r:

$$\upsilon_s = V_0 n \frac{r_0^2}{r^2},$$

where the parameter $n = r_s/r_0$ shows the remoteness of the satellite's orbit from the circulation core, and r_s is the distance from the center of the core to the orbit. The amplification coefficient (18), without considering the exponential multiplier, changes linearly relative to υ_s:

$$A(r) \approx 1 \pm \frac{\upsilon_s}{(\bar{U}_{xo} \mp V_0)n}.$$

Dependences of the amplification coefficient at different values of parameter n are shown in Fig. 4b. Considering the geometry of the intersection of the circulation region by the satellite, there is a linear dependence of the AGW amplitude on the wind velocity, which is in a close agreement with the experimental data.

CONCLUSIONS

The effect of intensification of AGW amplitudes in the polar thermosphere has been studied within the framework of a simple hydrodynamic model describing large-scale horizontal rotational motion of the medium.

We have considered the model of horizontal circulation of the thermosphere, which includes the inner region of the vortex and the extended region behind the core, where the rotation velocity decreases. We have studied the waves propagating along the circular lines of the current in the region of potential declining flow behind the core. As seen from Eq. (18), during the AGW motion in the direction opposite the flow, their amplitudes increase along the radius, depending on the velocity of the flow. At the same time, in favorable flow, the amplitudes of waves decrease. The maximum amplification of amplitudes occurs for

the waves for which $\bar{U}_x \to \upsilon_\varphi$ or $\bar{\omega} \to N$ in the reference frame of the moving medium, while the frequencies ω in the fixed observer reference frame are low. The change in amplitudes of the waves occurs predominantly on account of centrifugal forces of inertia. We have obtained an analytical expression for the coefficient of amplification of AGW amplitudes in the opposite wind. Numerical estimations of an increase in the amplitudes of perturbations carried out using the amplification coefficient are in a close agreement with the experimental data acquired with the "Dynamic Explorer 2" satellite.

ACKNOWLEDGMENTS

The work was carried out as part of the Targeted Comprehensive Program of the National Academy of Sciences of Ukraine in Space Research and project no. 6060 of the Ukrainian Center of Science and Technology.

REFERENCES

1. V. V. Akimenko and O. K. Cheremnykh, "Modeling of vortical flows on a background of 2-dim convective thermo-mass-exchange process," J. Autom. Inf. Sci. **36** (2), 64–80 (2004).
2. E. I. Kryuchkov and A. K. Fedorenko, "Peculiarities of energy transport in the atmosphere by acoustic gravity waves," Geomagn. Aeron. (Engl. Transl.) **52**, 235–241 (2012).
3. Yu. P. Ladikov-Roev and O. K. Cheremnykh, *Mathematical Models of Continuous Media* (Naukova Dumka, Kyiv, 2010) [in Russian].
4. Yu. P. Ladikov-Roev, O. K. Cheremnykh, A. K. Fedorenko, and V. E. Nabivach, "Acoustic-gravity waves in whirling polar thermosphere," J. Autom. Inf. Sci. **47** (9), 10–22 (2015).
5. M. G. Lighthill, *Waves in Fluids* (Cambridge Univ. Press, Cambridge, 1978; Mir, Moscow, 1981).
6. L. D. Landau and E. M. Lifshits, *A Course of Theoretical Physics*, Vol. 6: *Fluid Mechanics* (Nauka, Moscow, 1986; Pergamon, Oxford, 1987).
7. A. K. Fedorenko and E. I. Kryuchkov, "Distribution of medium-scale acoustic gravity waves in polar regions according to satellite measurement data," Geomagn. Aeron. (Engl. Transl.) **51**, 520–533 (2011).
8. A. K. Fedorenko and E. I. Kryuchkov, "Wind control of the propagation of acoustic gravity waves in the polar atmosphere," Geomagn. Aeron. (Engl. Transl.) **53**, 377–388 (2013).
9. O. K. Cheremnykh, "On the motion of vortex rings in an incompressible media," Nelineinaya Din. **4**, 417–428 (2008).
10. O. K. Cheremnykh, Yu. A. Selivanov, and I. V. Zakharov, "The effect of atmosphere's compressibility and non-isothermicity on the propagation of acoustic-gravity waves," Kosm. Nauka Tekhnol. **16**, 9–19 (2010).
11. A. K. Fedorenko, A. V. Bespalova, O. K. Cheremnykh, and E. I. Kryuchkov, "A dominant acoustic-gravity mode in the polar thermosphere," Ann. Geophys. **33**, 101–108 (2015).doi doi 10.5194/angeo-33-101-2015
12. D. C. Fritts and T. S. Lund, "Gravity wave in fluences in the thermosphere and ionosphere: Observations and recent modeling," in *Aeronomy of the Earth's Atmosphere and Iono-Sphere*, Ed. by M. A. Abdu, D. Pancheva, and A. Bhattacharyya (Springer-Verlag, Dordrecht, 2011). pp. 109–130. doi 10.1007/978-94-007-0326-18
13. C. O. Hines, "Internal atmospheric gravity waves at ionospheric heights," Can. J. Phys. **38**, 1441–1481 (1960).
14. R. D. Hunsucker, "Atmospheric gravity waves generated in the high-latitude ionosphere: A review," Rev. Geophys. Space Phys. **20**, 293–315 (1982).
15. T. L. Killeen, Y. I. Won, R. J. Nicieyewski, and A. G. Burns, "Upper thermosphere winds and temperatures in the geomagnetic polar cap: Solar cycle, geomagnetic activity, and interplanetary magnetic fields dependencies," J. Geophys. Res.: Space Phys. **100**, 21327–21342 (1995).
16. H. Lühr, S. Rentz, P. Ritter, H. Liu, K. Häusler, "Average thermospheric wind patterns over the polar regions, as observed by CHAMP," Ann. Geophys. **25**, 1093–1101 (2007). http://www.ann-geophys.net/25/1093/2007.
17. C. J. Nappo, *An Introduction to Atmospheric Gravity Waves* (Academic, San Diego, 2002).
18. Yu. G. Rapoport, O. K. Cheremnykh, Yu. A. Selivanov, A. K. Fedorenko, V. M. Ivchenko, V. V. Grimalsky, E. N. Tkachenko, "Modeling AGW and PEMW in inhomogeneous atmosphere and ionosphere," in *Proc. 2012 Int. Conf. of Mathematical Methods in Electromagnetic Theory (MMET 2012), Kharkiv, Ukraine, Aug. 28–30, 2012* (IEEE, 2012), pp. 577–580, paper id. 6331225.
19. S. L. Vadas and D. C. Fritts, "Thermospheric responses to gravity waves: Influences of increasing viscosity and thermal diffusivity," J. Geophys. Res.: Atmospheres **110**, D15103 (2005). doi 10.1029/2004JD005574
20. S. L. Vadas and M. J. Nicolls, "The phases and amplitudes of gravity waves propagating and dissipating in the thermosphere: Theory," J. Geophys. Res.: Space Phys. **117**, A05322 (2012). doi doi 10.1029/2011JA017426
21. E. Yiğit, A. S. Medvedev, A. D. Aylward, P. Hartogh, and M. J. Harris, "Modeling the effects of gravity wave momentum deposition on the general circulation above the turbopause," J. Geophys. Res.: Atmospheres **114**, D07101 (2009). doi 10.1029/2008JD011132
22. S. D. Zhang and F. Yi, "A numerical study of propagation characteristics of gravity wave packets propagating in a dissipative atmosphere," J. Geophys. Res.: Atmospheres **107**, 4222 (2002). doi 10.1029/2001JD000864

Translated by M. Chubarova